Implications of the Coherence Length on the Discrete Wigner Potential

P. Ellinghaus, M. Nedjalkov, and S. Selberherr
Institute for Microelectronics, TU Wien, Gußhausstraße 27–29/E360, 1040 Wien, Austria
E-mail: {ellinghaus | nedjalkov | selberherr}@iue.tuwien.ac.at

I. Introduction

The solution of the Wigner equation, using the Monte Carlo method [1] along with the signed-particle technique [2], requires a finite coherence length to be chosen. We investigate how the choice of the coherence length influences computational aspects of the calculation of the Wigner potential, like momentum resolution. Additionally, the physical interpretation attributed to a chosen coherence length is discussed.

Firstly, we define the semi-discrete Wigner potential:

$$V_W(\mathbf{r},\mathbf{P}) \equiv \frac{1}{i\hbar\mathbf{L}} \int_{-\mathbf{L}/2}^{\mathbf{L}/2} d\mathbf{s}\, e^{-i2\mathbf{P}\Delta\mathbf{k}\cdot\mathbf{s}} \delta V$$
$$\delta V(\mathbf{s};\mathbf{r}) \equiv V(\mathbf{r}+\mathbf{s}) - V(\mathbf{r}-\mathbf{s}), \tag{1}$$

where the position vectors, $\mathbf{r}$ and $\mathbf{s}$, are bounded by the (active) device length, $\mathbf{L}_{dev}$, and the coherence length, $\mathbf{L}$, respectively. The momentum vector, $\mathbf{P}\Delta\mathbf{k}$, is discretized in steps of $\Delta\mathbf{k} = \frac{\pi}{\mathbf{L}}$, which makes the full discretization of (1) akin to a discrete Fourier transform (DFT) of the potential difference. For the illustrative, one-dimensional case, the discrete Wigner potential used for numerical simulations is therefore defined as

$$V_W(m,p) = \frac{1}{i\hbar N} \sum_{n=0}^{N-1} e^{-i2\left(pn\frac{\pi}{N}\right)}$$
$$V\left(m\Delta x + \left(n-\frac{N}{2}\right)\Delta s\right) - V\left(m\Delta x - \left(n-\frac{N}{2}\right)\Delta s\right). \tag{2}$$

II. Computational aspects

It is desirable to choose the coherence length as short as possible to limit the computational load of calculating the Wigner potential, which can be substantial in multi-dimensional simulations. However, the coherence length also determines the momentum resolution Δk, therefore, $\mathbf{L}$ must be chosen sufficiently large to be able to differentiate the spectral content of different potential profiles. The attainable momentum resolution is also subject to the device dimensions, which place an upper bound on $\mathbf{L}$.

Fig. 1 shows different analytical potential profiles of the form

$$V(x) = V_0 + mx + V_1 \sin \omega x, \tag{3}$$

which suggest a sinusoidal potential variation, with a spatial frequency ω, superimposed on a potential bias ($V_0 + mx$). Since ω can be chosen, the bins (values of momentum index p) of the corresponding Wigner potential (2), which should be non-zero, are known. If ω is chosen ($\omega = 1.0, 1.8$; *cf.* Fig. 1) such that only the bins 1 and 2 of the corresponding Wigner potentials (at a fixed position) should be non-zero, Fig. 2 reveals that this is not the case – there appear non-zero values at much higher-valued bins. These values at higher bins are not attributable to the physical profile, but are due to adverse effects, often termed 'spectral leakage', inherent when calculating a DFT of a non-periodic 'function' over a finite length [3]. This situation is further exacerbated by the biasing condition which introduces a big discontinuity, because, when calculating the DFT, the potential profile is implicitly assumed to repeat periodically.

When using the signed-particle method to solve the Wigner equation [2], the Wigner potential is normalized to represent a probability distribution for the generation of particles with a given momentum offset $\mathbf{P}$ (negative values of V_w represent a negative offset; $-V_W(\cdot,\mathbf{P}) = V_W(\cdot,-\mathbf{P})$). In the context of this physical interpretation of the Wigner potential, the accumulated probability of the higher-valued bins becomes significant and causes the generation of particles with very high momenta, which cannot be attributed to the physical potential in the 'device'. A distribution, much better representing the physical profiles is attained, if we apply a Tukey window function [4] to taper the potential profile at the boundaries towards zero, thereby remedying the discontinuities introduced by the periodic repetition of the potential profile, which is implied when calculating a DFT. Amongst the plethora of available window functions [3] – also known as tapering functions – the Tukey window (with $\alpha = 0.2$; *cf.* Fig. 3) was

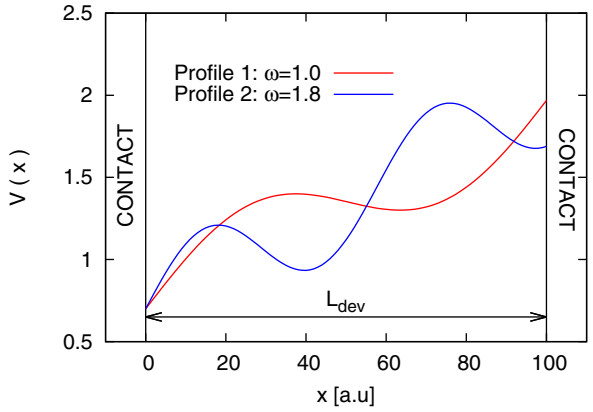

Fig. 1. Two analytic potential profiles, of the form (3), with known spectral content (ω) and a bias between the left and the right contacts of 1.3 V.

978-1-4799-5433-9/14/$31.00 © 2014 IEEE

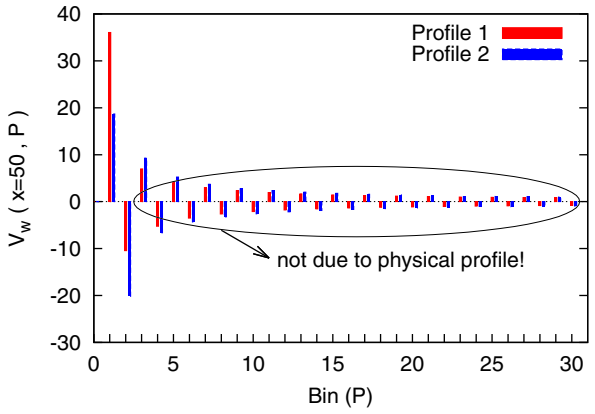

Fig. 2. Wigner potential at a fixed position, $V_W\ (x = 50, P)$, for the profiles in Fig. 1, calculated with a coherence length of $\mathbf{L} = \mathbf{L}_{dev}$.

chosen with the physical motivation that it does not alter the physical profile inside the device noticably. Fig. 4 shows that by applying the Tukey window the (unphysical) higher bin values are suppressed, while the actual spectral components of the profile, at bins 1 and 2, remain pronounced. This results in a relative change of the probability distribution (Fig. 5), which better reflects the physical situation in the device, by highlighting the bins the actual potential should influence. Ultimately, this also substantially improves the accuracy of the solution of the Wigner equation [5].

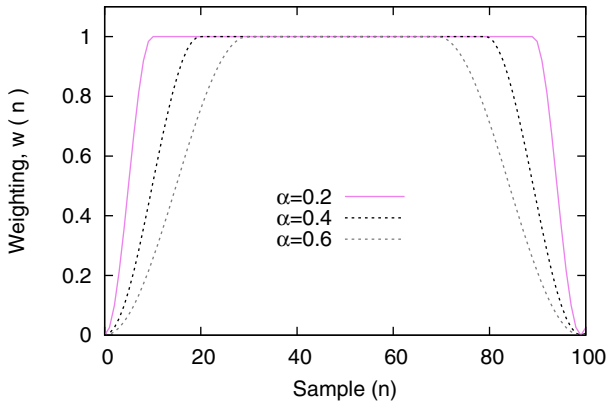

Fig. 3. Tukey window function, for various values of α, used to smooth the potential values toward zero at the boundaries by appropriately weighting the samples (potential difference values) used to compute the DFT in the Wigner potential.

III. Physical Interpretation

Apart from the computational considerations and implications of choosing a finite coherence length, physical considerations must also be made; several physical interpretations are possible: If decoherence effects are not modeled through the choice of $\mathbf{L}$ itself [6] – e.g. [7] considers an exponential damping which essentially reduces $\mathbf{L}$ to model decoherence – the coherence length should be chosen to (at least) cover the extent of the device at every point, where the Wigner potential is calculated, such that the entire potential profile is considered; this implies $\mathbf{L} \geq 2\mathbf{L}_{dev}$. However, under the physical assumption that no coherence exists between the contacts, we must adopt $\mathbf{L} = \mathbf{L}_{dev}$. This considerably reduces

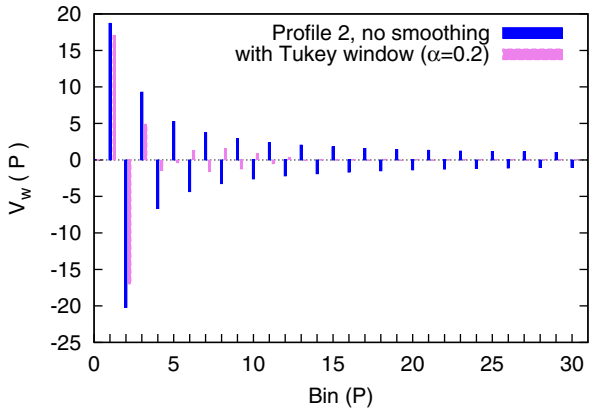

Fig. 4. The unnormalized Wigner potential, $V_W\ (x = 50, P)$, calculated at the centre of the device with and without the application of a smoothing Tukey window ($\alpha = 0.2$), using Profile 2 (blue) in Fig. 1, and a coherence length of $\mathbf{L} = \mathbf{L}_{dev}$.

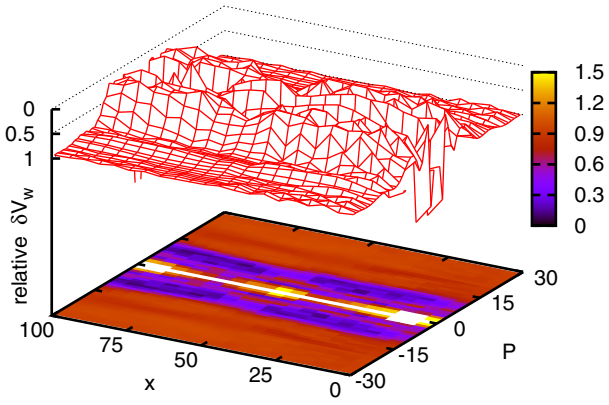

Fig. 5. The relative absolute difference of the probability distributions (normalized WPs) calculated with and without the application of a smoothing Tukey window ($\alpha = 0.2$), using Profile 2 (blue) in Fig. 1. A coherence length of $\mathbf{L} = \mathbf{L}_{dev}$ is used, along with boundary approach i) discussed in the text.

the computational burden of calculating the Wigner potential and is also justified, if the modeled decoherence processes reduce the effective coherence length sufficiently. Nonetheless, when calculating (1) at any point other than the center of the device, i.e. $V_W\left(\mathbf{r} \neq \frac{\mathbf{L}}{2}, \cdot\right)$, the boundaries of the device are exceeded and therefore the potential is unknown.

Two limiting approaches to treat this situation are to i) regard any point outside the device to be in a contact region, which is assumed to maintain equilibrium conditions, and extend the potential value at the boundary as a constant, or to ii) assume no coherence exists between the device and the contact region outside, and progressively reduce the coherence length as the boundary is approached. Fig. 6 reveals that the difference between these two approaches is significant. Approach ii) implies a decreasing value of Δk as the boundary is approached. To efficiently interpolate the values onto the fixed, finer, momentum grid, the potential difference in (1) is zero-padded at the front and the back. A further consideration when using approach ii) is that a shrinking coherence length implies that the portion of the potential profile considered for calculating the Wigner potential gradually reduces as the boudary is approached, up to the point, where the Wigner po-

tential is no longer predominantly determined by the potential profile, but rather the length/width of the 'coherence box' – a rectangular window with undesirable effects, as discussed before.

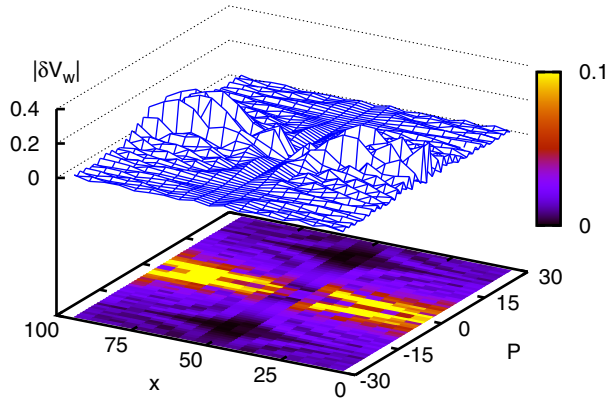

Fig. 6. The absolute value of the difference of the (normalized) WPs corresponding to the different boundary treatments (discussed in text), using Profile 2 (blue) in Fig. 1.

IV. Conclusion

It is evident that the choice of a finite coherence length is not at all trivial and is subject to both computational and physical considerations. We have highlighted some of the implications a finite coherence length has on the numerical computation of the Wigner potential along with possible treatments to attain more physically-sound solutions of the Wigner equation. The choice of the coherence length and the associated boundary conditions remains a challenging research topic [8] and, ultimately, reflects the physical interpretation, which has been adopted.

Acknowledgement

This work has been supported by the Austrian Science Fund, project FWF-P21685-N22.

References

[1] I. T. Dimov, *Monte Carlo Methods for Applied Scientists*. World Scientific, 2008.

[2] M. Nedjalkov and D. Vasileska, "Semi-discrete 2D Wigner-particle approach," *Journal of Computational Electronics*, vol. 7, no. 3, pp. 222–225, 2008.

[3] F. Harris, "On the use of windows for harmonic analysis with the discrete Fourier transform," *Proceedings of the IEEE*, vol. 66, no. 1, pp. 51–83, Jan 1978.

[4] J. W. Tukey, "An introduction to the calculation of numerical spectrum analysis," *Spectral Analysis of Time Series*, pp. 22–46, 1967.

[5] P. Ellinghaus, M. Nedjalkov, and S. Selberherr, "The Wigner Monte Carlo method for accurate semiconductor device simulation," Proc. of the 19th Int. Conf. on Simulation of Semiconductor Processes and Devices (SISPAD), Sep 2014, to be published.

[6] M. Nedjalkov, S. Selberherr, D. Ferry, D. Vasileska, P. Dollfus, D. Querlioz, I. Dimov, and P. Schwaha, "Physical scales in the Wigner-Boltzmann equation," *Annals of Physics*, vol. 328, pp. 220–237, 2012.

[7] C. Jacoboni and P. Bordone, "Wigner transport equation with finite coherence length," *Journal of Computational Electronics*, vol. 13, no. 1, pp. 257–263, 2014.

[8] R. Rosati, F. Dolcini, R. C. Iotti, and F. Rossi, "Wigner-function formalism applied to semiconductor quantum devices: Failure of the conventional boundary condition scheme," *Phys. Rev. B*, vol. 88, p. 035401, Jul 2013.